AIMS Mathematics, 10(7): 16291–16316.
DOI: 10.3934/math.2025728
Received: 17 April 2025
Revised: 03 July 2025
Accepted: 04 July 2025
Published: 18 July 2025

https://www.aimspress.com/journal/Math

Research article

Mathematical and numerical analysis of a SEVIR-S model for adenovirus with immunity waning and reinfection effects

Rabeb Sidaoui[1], W. Eltayeb Ahmed[2], Arshad Ali[3], Mohammed Rabih[4,*], Amer Alsulami[5], Khaled Aldwoah[6,*] and E. I. Hassan[2]

[1] Department of Mathematics, College of Science, University of Ha'il, 55473 Ha'il, Saudi Arabia

[2] Department of Mathematics and Statistics, Imam Mohammad Ibn Saud Islamic University (IMSIU), Riyadh 13318, Saudi Arabia

[3] Department of Mathematics, University of Malakand, Lower Dir, Chakdara 18000, Khyber Pakhtunkhwa, Pakistan

[4] Department of Mathematics, College of Science, Qassim University, Buraydah 51452, Saudi Arabia

[5] Department of Mathematics, Turabah University College, Taif University, Taif, Saudi Arabia

[6] Department of Mathematics, Faculty of Science, Islamic University of Madinah, Madinah 42351, Saudi Arabia

* **Correspondence:** Email: m.fadlallah@qu.edu.sa, aldwoah@iu.edu.sa.

Abstract: In this study, we proposed a modified SEVIR-S (susceptible, exposed, vaccinated, infected, recovered) model for the transmission dynamics of adenovirus by incorporating the effects of immunity waning and reinfection. Unlike the classical SEVIR framework, the extended model accounted for the possibility that recovered individuals may lose immunity over time and become susceptible again — a critical feature for accurately modeling diseases like adenovirus. To better capture the disease's memory effects and temporal dynamics, the model used the fractal-fractional Caputo-Fabrizio derivative with a power-law kernel. The paper analyzed the model's existence and stability using fixed point theory and Hyers-Ulam (H-U) stability. Furthermore, both the disease-free and endemic equilibrium points and their stability were analyzed. Also, the basic reproduction number was provided. The findings were validated through numerical simulations using an extended Adams-Bashforth method.

Keywords: SEVIR-S model; adenovirus transmission; immunity waning and reinfection; disease-free and endemic equilibria; model existence and stability; approximate solution; simulations
Mathematics Subject Classification: 26A33, 34A08, 34A12

1. Introduction

Common viral pathogens like adenovirus, which are members of the Adenoviridae family, can cause a variety of illnesses such as gastrointestinal, ophthalmic, and respiratory infections. Adenovirus transmission is a major contributor to infectious conjunctivitis in humans. This condition results from inflammation affecting the conjunctiva, which lines the inside of the eyelids and covers the white part of the eye. The inflammation can be triggered by viral, bacterial, or allergic factors. Humans may experience various forms of conjunctivitis. For instance, allergic conjunctivitis can arise due to seasonal exposure to allergens or irritants such as pollen, dust mites, animal dander, contact lenses, or certain chemicals [1, 2]. The disease typically spreads when an infected individual comes into direct or indirect contact with someone who is susceptible. This interaction entails coming into contact with contaminated objects. This contact involves coming into contact with contaminated objects that have fallen into the eyes as well as being exposed to discharge from the upper respiratory tracts or conjunctivae of sick people. There is also a suggestion that there is a direct link between the risk of mother-to-child transmission in newborns and maternal chlamydia and gonococcal infections.

The acute hemorrhagic conjunctivitis (AHC) is a viral form of eye inflammation. The disease typically has an incubation period ranging from one to three days. Common symptoms include tearing, sore throat, eye irritation, and sensitivity to light, often accompanied by eyelid swelling or purulent discharge [3]. Effective strategies to reduce the spread of AHC involve the use of antibiotic eye drops, maintaining proper hygiene, patient isolation, and allowing the infection to resolve naturally, which usually takes between two and three weeks. The incidence of conjunctivitis is notably higher in tropical climates [4, 5], with a particular increase during the rainy season when elevated humidity levels promote viral activity [6]. For instance, in tropical countries such as Thailand, the disease is frequently reported [7, 8]. Isolating infected individuals is an important step in minimizing further transmission [9]. Moreover, encouraging home isolation through sick leave not only supports faster recovery but also limits potential exposure to others [9].

According to the American Academy of Pediatrics, children should refrain from attending school during the infectious period to minimize close contact with peers and slow disease transmission (David et al., 2015). The development of mathematical models has significantly enhanced our understanding of AHC dynamics. Noteworthy contributions in this area include the works in [6, 10–12].

In [6], the authors formulated conjunctivitis disease with classical derivatives as follows

$$\begin{cases} \dfrac{dS}{dt} = Nb_r - d_r S(\tau) - \delta I(\tau) S(\tau), \\ \dfrac{dE}{dt} = \delta I(\tau) S(\tau) - d_r E(\tau) - kE(\tau), \\ \dfrac{dI}{dt} = kE(\tau) - d_r I(\tau) - (p+q) I(\tau), \\ \dfrac{dR}{dt} = (p+q) I(\tau) - d_r R(\tau), \\ S(0) = S_0, E(0) = E_0, I(0) = I_0, R(0) = R_0. \end{cases} \tag{1.1}$$

In the SEIR model given in (1.1), the compartment "S" represents individuals who are susceptible, "E" denotes those who have been exposed, "I" corresponds to individuals infected with conjunctivitis, and "R" indicates those who have recovered. The remaining parameters are detailed in Table 1. In [13],

the authors included a vaccinated class V in the model and formulated it in Atangana-Baleanu-Caputo sense as described by:

$$\begin{cases} {}^{ABC}D_{\tau}^{\sigma}S(\tau) = Nb_r - \delta IS(\tau) - d_rS(\tau), \\ {}^{ABC}D_{\tau}^{\sigma}E(\tau) = \delta IS(\tau) - \gamma E(\tau) - d_rE(\tau), \\ {}^{ABC}D_{\tau}^{\sigma}V(\tau) = \gamma E(\tau) - \beta V(\tau) - d_rV(\tau), \\ {}^{ABC}D_{\tau}^{\sigma}I(\tau) = \beta V(\tau) - (p+q+d_r)I(\tau), \\ {}^{ABC}D_{\tau}^{\sigma}R(\tau) = (p+q)I(\tau) - d_rR(\tau), \\ S(0) = S_0, E(0) = E_0, V(0) = V_0, I(0) = I_0, R(0) = R_0, \end{cases} \tag{1.2}$$

where the notation ${}^{ABC}D_{\tau}^{\sigma}$ denotes the Atangana-Baleanu-Caputo fractional derivative of order σ. This model is now referred to as SEVIR, where V represents the vaccinated class while S, E, I, and R are already defined above.

Table 1. Parameters and their description.

Parameters	Definition	Parameters values
N	Total population	1000
δ	transmission rate for Acute Hemorrhagic Conjunctivitis (AHC)	0.001127
b_r	Birth rate	0.001190
d_r	Natural death rate	0.00060101
ω	Protection lose rate of vaccinated individuals	0.001170
μ	Immunity lose rate of recovered individuals	0.000220
γ	Incubation rate for AHC	0.1517
β	Incidence rate from vaccinated compartment to infected compartment	0.01107
p	Recovered rate for symptomatic individuals	0.1330
q	Quarantine rate for symptomatic individuals	0.1700

The parameter values in Table 1 have been assumed based on biologically plausible ranges to facilitate the qualitative analysis of the model.

Similarly, in [14], Nisar et al. studied model (1.2) in sense of the Caputo fractional differential operator and investigated a detailed analysis of the model with treatment impact.

Biological sciences have experienced significant growth over the past few decades, and it is realistic to anticipate that this development will continue due to major technological breakthroughs. Mathematics has continuously benefited society and brought about significant advances. Similar to how mathematics has revolutionized the natural sciences, it has the potential to transform biological research [15]. Mathematical models enable us to comprehend the fascinating complexity that biology presents, and biology evaluates these mathematical representations in turn. Complex mathematical problems are now easier to handle thanks to recent advances in computer algebra systems. Consequently, this frees up researchers to concentrate on understanding mathematical biology instead of figuring out how to solve problems [16]. Several numerical methods are used to approximate solutions to complex mathematical problems that may not have an analytical solution. We refer to some numerical results in [17, 18]. The mathematical simulation of several biological, physical, and epibiological phenomena has garnered attention in recent times. In [19], the authors employ analytical

techniques to analyze the behavior of the model and derive meaningful insights into the progression of breast cancer. In [20], the authors explored the dynamics of a waterborne disease model using fractal-fractional calculus. The study investigates the theoretical and numerical aspects of the model's solutions, employing simulations to gain insights into the behavior of the system. In [21], the authors presented a fractal fractional-order model to investigate the dynamics of liver fibrosis disease. They derived mathematical results for the model, with focusing on subinterval transitions. Similarly, using a Φ-piecewise hybrid fractional derivative approach, the authors studied the dynamics of the Ebola disease model [22]. The main reason for this increase in interest is the power of mathematical models.

The majority of biological diseases are first modeled using classical derivatives. There has been a change in interest from classical calculus to fractional calculus as a result of recent developments in mathematics and its applications. To enhance the accuracy of mathematical models, especially in the context of real-world phenomena, researchers in applied mathematics have increasingly turned to the tools of fractional calculus. We refer to [23–25]. In [26], the authors demonstrated the application of fractional calculus for dynamic problems. The field of fractional calculus is constantly evolving in order to fully and precisely comprehend the characteristics of practical issues. It enables scientists working in this area to examine and investigate phenomena that integer order calculus is unable to adequately express. The application of fractional derivatives and integrals can aid in the understanding of complex systems and phenomena. The development of fractional-order calculus offers an opportunity to deepen our understanding of practical problems. Caputo and Fabrizio introduced a novel type of fractional derivative characterized by a non-singular kernel, which has contributed significantly to the advancement of fractional differential equations; see [27].

The most recent developments in fractional calculus occurred due to the concept of fractals and fractional order derivatives and integrals, which were originally introduced explicitly a few years ago by author [28], despite the fact that the idea of fractals predates fractional calculus. Fractals and fractional analysis have been applied by researchers to study a variety of physical scientific issues. See, for example, [29], and [30].

Applying the fractal-fractional Caputo-Fabrizio (FFCF) derivative in the mathematical modeling of infectious diseases, such as adenovirus transmission, introduces several key benefits beyond those offered by traditional integer-order and standard fractional models. One notable feature of the FFCF operator is its use of a non-singular kernel, which circumvents the numerical and conceptual challenges posed by the singular kernels in classical Caputo or Riemann-Liouville formulations. This contributes to more stable computations and aligns better with physical processes characterized by exponentially fading memory. The smooth memory representation intrinsic to the Caputo-Fabrizio kernel ensures consistent and robust results, particularly when simulating over extended time periods–crucial for understanding long-term epidemiological trends involving gradual immunity loss and repeated exposure.

Incorporating a fractal structure further enhances the model's capacity by accounting for irregular spatial or contact patterns often found in real-world populations, where uniform mixing is an unrealistic assumption. This integration of the fractal dimension allows the model to better reflect heterogeneous interactions within a population. Moreover, the FFCF model includes two adjustable parameters: the fractional order, which governs how past states influence present dynamics, and the fractal dimension, which characterizes spatial irregularities. Together, they offer a highly adaptable modeling framework capable of capturing delayed infection peaks, multiple epidemic waves, and complex spatial

transmission.

The SEVIR-S framework, which integrates aspects like waning immunity and reinfection, aligns well with adenovirus behavior, where immunity is temporary and reinfections are frequent. The FFCF formulation effectively captures the gradual, non-instantaneous nature of immunity decline-something that conventional integer-order models struggle to represent adequately.

In this research, we modify the proposed model by considering immunity waning and reinfection. We present our modified model by:

$$\begin{cases} {}^{FFCF}D_{\tau}^{\sigma,\varrho}S(\tau) = Nb_r - \delta IS(\tau) - d_rS(\tau) + \omega V(\tau) + \mu R(\tau), \\ {}^{FFCF}D_{\tau}^{\sigma,\varrho}E(\tau) = \delta IS(\tau) - \gamma E(\tau) - d_rE(\tau), \\ {}^{FFCF}D_{\tau}^{\sigma,\varrho}V(\tau) = \gamma E(\tau) - \beta V(\tau) - d_rV(\tau) - \omega V(\tau), \\ {}^{FFCF}D_{\tau}^{\sigma,\varrho}I(\tau) = \beta V(\tau) - (p+q+d_r)I(\tau), \\ {}^{FFCF}D_{\tau}^{\sigma,\varrho}R(\tau) = (p+q)I(\tau) - d_rR(\tau) - \mu R(\tau), \\ S(0) = S_0, E(0) = E_0, V(0) = V_0, I(0) = I_0, R(0) = R_0, \end{cases} \tag{1.3}$$

where the notation ${}^{FFCF}D_{\tau}^{\sigma,\varrho}$ represents the Caputo-Fabrizio fractal-fractional derivative of fractional order σ and fractal dimension ϱ, while ω is the vaccine waning rate and μ is the immunity waning rate.

The modified SEVIR-S model for adenovirus spread with immunity waning and reinfection offers several advantages over the standard SEVIR model: Unlike the traditional SEVIR model, this extension considers reinfection, which is crucial for diseases like adenovirus where immunity may not be permanent. By introducing an immunity waning parameter, the model reflects real-world scenarios where recovered individuals can lose immunity over time. Moreover, this model provides a more comprehensive understanding of long-term disease persistence and helps to determine whether reinfection alters the stability of disease-free and endemic equilibria which is crucial for designing long-term interventions.

Due to the presence of the FFCF derivative in the proposed model, which incorporates both memory effects and nonlocal characteristics through its non-singular kernel, traditional approaches for classical differential equations may not be sufficient. These distinctive features require an independent mathematical investigation to guarantee that the model is well-defined and solvable. Therefore, we conduct an analysis of existence, uniqueness, and stability of the solutions by applying fixed point methods within a suitably chosen functional framework.

2. Basic results

In the following section, we present the necessary theoretical background and analytical tools. These include definitions from fractal-fractional calculus involving FFCF derivatives and fractal-fractional Riemann-Liouville (FFRL) integrals with various kernels.

Definition 2.1. [28] Let $\xi(\tau)$ be a continuous function that is fractally differentiable on the interval (a, b) of order ϱ. Then, its FFCF derivative of order σ with an exponential decay kernel is given as:

$${}^{FFCF}D^{\sigma,\varrho}\xi(\tau) = \frac{M(\sigma)}{1-\sigma}\int_0^{\tau}\frac{d}{dy^{\varrho}}\xi(y)\exp\Big(-\frac{\sigma}{1-\sigma}(\tau-y)\Big)dy, \quad \tau \in [0,T], \tag{2.1}$$

where $0 < \sigma, \varrho \leq 1$, $M(\sigma)$ is a normalization function such that $M(0) = M(1) = 1$, and

$$\frac{d}{dy^{\varrho}}\xi(y) = \lim_{\tau \to y} \frac{\xi(\tau) - \xi(y)}{\tau^{\varrho} - y^{\varrho}}. \tag{2.2}$$

Definition 2.2. [28] Let $\xi(\tau)$ be a continuous function that is fractally differentiable on the interval (a, b) of order ϱ. Then, its FFCF derivative of order σ is defined using a power-law kernel:

$${}^{FFCF}D^{\sigma,\varrho}\xi(\tau) = \frac{1}{\Gamma(1-\sigma)} \int_0^{\tau} \frac{d}{dy^{\varrho}}\xi(y)(\tau - y)^{-\sigma} dy, \quad \tau \in [0, T], \tag{2.3}$$

where $0 < \sigma, \varrho \leq 1$.

Definition 2.3. [28] Let $\xi \in C(0, T)$ then the FFRL integral of the function $\xi(\tau)$ with an exponential decay kernel is given by

$${}^{FFRL}I^{\sigma,\varrho}\xi(\tau) = \frac{\varrho(1-\sigma)\tau^{\varrho-1}\xi(\tau)}{M(\sigma)} + \frac{\sigma\varrho}{M(\sigma)} \int_a^{\tau} y^{\sigma-1}\xi(y)dy. \tag{2.4}$$

Definition 2.4. [28] Let $\xi \in C(0, T)$ then the FFRL integral of the function $\xi(\tau)$ with power-law kernel is given as

$${}^{FFRL}I^{\sigma,\varrho}\xi(\tau) = \frac{\varrho}{\Gamma(\sigma)} \int_a^{\tau} (\tau - y)^{\sigma-1} y^{\varrho-1}\xi(y)dy. \tag{2.5}$$

Definition 2.5. [31] A set Z of real valued continuous functions defined on a domain $D \subseteq \mathbb{R}$ is called equi-continuous on the domain D if, for every $\epsilon > 0$, there exists a $\zeta > 0$ such that for all $x \in Z$ and any $t_1, t_2 \in D$ with $|t_1 - t_2| < \zeta$, the following condition

$$|x(t_1) - x(t_2)| < \epsilon,$$

is satisfied.

The definition is extended to operator as:

Definition 2.6. Let T be an operator mapping a normed space V into another normed space X. The operator T is called equi-continuous if, for every $\epsilon > 0$, there exists a $\zeta > 0$ such that all $t_1, t_2 \in V$ with $\|t_1 - t_2\|_V < \zeta$, and the inequality

$$\|T(t_1) - T(t_2)\|_X < \epsilon$$

holds.

This property is critical in applying the Arzelà-Ascoli theorem.

Theorem 2.1. *(Krasnoselskii's fixed point theorem) [32] Let $(\mathbb{X}, \|.\|)$ be a Banach space and let $\mathfrak{B}$ be its nonempty closed convex subset. Let $\mathbb{Q}_1$ and $\mathbb{Q}_2$ be the two operators that map $\mathfrak{B}$ into $\mathbb{X}$ such that*

- *$\mathbb{Q}_1 x + \mathbb{Q}_2 y$ whenever $x, y \in \mathfrak{B}$;*
- *$\mathbb{Q}_1$ is a contraction mapping;*
- *$\mathbb{Q}_2$ is a continuous and compact.*

Then there exists $z \in \mathfrak{B}$ *such that* $z = \mathbb{Q}_1 z + \mathbb{Q}_2 z$.

Definition 2.7. The Adams-Bashforth method for solving ordinary differential equations numerically can be described by the following scheme:

$$x_{\ell+1} = x_\ell + h \sum_{i=0}^{r-1} a_i f(t_{\ell-i}, x_{\ell-i}),$$

where x_ℓ represents the numerical approximation at time t_ℓ, and $t_\ell \in [0, K-1]$, with $K = \frac{T}{h}$, where T is the final time and h the time step size, $f(x, \xi)$ is the given ordinary differential equation and a_i are method-specific coefficients that depend on the order of the method.

3. Derivation of the model

In this part, we first derive a classical integer order model of the conjunctivitis viral illness. We next apply it to the mathematical model of fractal-fractional that has been proposed. The entire population $N(\tau)$ is classified into five compartments, i.e., $N(\tau) = S(\tau) + E(\tau) + V(\tau) + I(\tau) + R(\tau)$.

Susceptible compartment: The susceptible compartment or class increases due to births at a rate b_r from the total population N, loss of immunity at a rate ω from the vaccinated group V, and reinfection at a rate μ from the recovered group R. It declines at a rate d_r as a result of mortality. Also, it declines at a rate δ from contact between I and S due to infections. Therefore, the formulated dynamics of the class $S(\tau)$ are

$$\frac{dS(\tau)}{dt} = Nb_r - \delta IS(\tau) - d_r S(\tau) + \omega V(\tau) + \mu R(\tau). \tag{3.1}$$

Exposed compartment: This class gains individuals through infections at a rate δ from interactions between I and S, while it loses individuals due to natural deaths at rate d_r and through progression to the exposed class at an incubation rate γ. Hence, the dynamics of the class are formulated by

$$\frac{dE(\tau)}{dt} = \delta IS(\tau) - \gamma E(\tau) - d_r E(\tau). \tag{3.2}$$

Vaccinated compartment: The class $V(\tau)$ is recruited at the incubation rate γ of the exposed population and is decreased by a natural fatality rate d_r. It is also reduced by the incidence rate β and immunity waning rate ω. Therefore, the formulated dynamics of the class are given by

$$\frac{dV(\tau)}{dt} = \gamma E(\tau) - \beta V(\tau) - d_r V(\tau) - \omega V(\tau). \tag{3.3}$$

Infected compartment: The infected class $I(\tau)$ increases through recruitment at the rate β from $V(\tau)$ and is decreased by a natural fatality rate d_r. It is also reduced at the incidence rates p and q. Therefore, the formulated dynamics of the class are given by

$$\frac{dI(\tau)}{dt} = \beta V(\tau) - d_r I(\tau) - (p+q) I(\tau). \tag{3.4}$$

Recovered compartment: The recovered class grows due to recovery and disease-induced death, represented by the rates p and q, respectively, and decreases through natural mortality at rate d_r and reinfection rate μ. Therefore, the formulated dynamics of the class are provided by

$$\frac{dR(\tau)}{dt} = (p+q) I(\tau) - d_r R(\tau) - \mu R(\tau). \tag{3.5}$$

Using the formulated results given in (3.1), (3.2), (3.4), and (3.5), we obtain the following integer-order model of the spread of the adenovirus disease in human eyes as presented.

$$\begin{cases} \dfrac{dS}{dt} = Nb_r - \delta IS(\tau) - d_r S(\tau) + \omega V(\tau) + \mu R(\tau), \\ \dfrac{dE}{dt} = \delta IS(\tau) - \gamma E(\tau) - d_r E(\tau), \\ \dfrac{dV}{dt} = \gamma E(\tau) - \beta V(\tau) - d_r V(\tau) - \omega V(\tau), \\ \dfrac{dI}{dt} = \beta V(\tau) - (p + q + d_r) I(\tau), \\ \dfrac{dR}{dt} = (p + q) I(\tau) - d_r R(\tau) - \mu R(\tau). \end{cases} \tag{3.6}$$

4. Equilibrium points and basic reproduction number

In this part, we analyze disease-free equilibrium (DFE) and compute the basic reproduction number R_0.

To determine the equilibrium points, we set all the righthand sides of the differential equations in the system to zero.

$$\begin{cases} Nb_r - \delta IS - d_r S + \omega V + \mu R = 0, \\ \delta IS - \gamma E - d_r E = 0, \\ \gamma E - \beta V - d_r V - \omega V = 0, \\ \beta V - (p + q + d_r) I = 0, \\ (p + q) I - d_r R - \mu R = 0. \end{cases} \tag{4.1}$$

(1) DFE

At the DFE, there is no infection in the population, and, hence, we get

$$S^0 = \frac{Nb_r}{d_r}. \tag{4.2}$$

Thus, we have the following DFE:

$$(S^0, E^0, V^0, I^0, R^0) = \left(\frac{Nb_r}{d_r}, 0, 0, 0, 0 \right).$$

(2) Endemic equilibrium (EE)

The numerical EE point is given by

$$(S^*, E^*, V^*, I^*, R^*) \approx (316.2424, 24.3973, 94.9978, 3.4638, 561.1269).$$

Basic reproduction number:

As in [13], using the next-generation matrix approach, the basic reproduction number R_0 is derived as

$$R_0 = \frac{\delta S^0 \beta \gamma}{(\gamma + d_r)(\beta + d_r + \omega)(p + q + d_r)}. \tag{4.3}$$

At the DFE, $I^* = 0$ and $S^0 = \frac{Nb_r}{d_r}$, thus:

$$R_0 = \frac{\delta N b_r \beta \gamma}{d_r(\gamma + d_r)(\beta + d_r + \omega)(p + q + d_r)}. \tag{4.4}$$

This is the expression for R_0, which determines whether the infection will spread in the population. If $R_0 > 1$, an epidemic occurs; otherwise, the disease will die out.

To discuss the stability at equilibrium points, we compute the Jacobian matrix as given below

$$J = \begin{bmatrix} \frac{\partial f_1}{\partial S} & \frac{\partial f_1}{\partial E} & \frac{\partial f_1}{\partial V} & \frac{\partial f_1}{\partial I} & \frac{\partial f_1}{\partial R} \\ \frac{\partial f_2}{\partial S} & \frac{\partial f_2}{\partial E} & \frac{\partial f_2}{\partial V} & \frac{\partial f_2}{\partial I} & \frac{\partial f_2}{\partial R} \\ \frac{\partial f_3}{\partial S} & \frac{\partial f_3}{\partial E} & \frac{\partial f_3}{\partial V} & \frac{\partial f_3}{\partial I} & \frac{\partial f_3}{\partial R} \\ \frac{\partial f_4}{\partial S} & \frac{\partial f_4}{\partial E} & \frac{\partial f_4}{\partial V} & \frac{\partial f_4}{\partial I} & \frac{\partial f_4}{\partial R} \\ \frac{\partial f_5}{\partial S} & \frac{\partial f_5}{\partial E} & \frac{\partial f_5}{\partial V} & \frac{\partial f_5}{\partial I} & \frac{\partial f_5}{\partial R} \end{bmatrix}. \tag{4.5}$$

Computing the partial derivatives:

$$J = \begin{bmatrix} -d - I\delta & 0 & \omega & -S\delta & \mu \\ I\delta & -d - \gamma & 0 & S\delta & 0 \\ 0 & \gamma & -\beta - d - \omega & 0 & 0 \\ 0 & 0 & \beta & -d - p - q & 0 \\ 0 & 0 & 0 & p + q & -d - \mu \end{bmatrix}. \tag{4.6}$$

At E_0, it will be

$$J_0 = \begin{bmatrix} -d_r & 0 & \omega & -\frac{\delta N b_r}{d_r} & \mu \\ 0 & -d_r - \gamma & 0 & \frac{\delta N b_r}{d_r} & 0 \\ 0 & \gamma & -\beta - d_r - \omega & 0 & 0 \\ 0 & 0 & \beta & -d_r - p - q & 0 \\ 0 & 0 & 0 & p + q & -d_r - \mu \end{bmatrix}. \tag{4.7}$$

The characteristic equation is given by

$$\left| J_0 - \Upsilon I \right| = \begin{vmatrix} -\Upsilon - d_r & 0 & \omega & -\frac{\delta N b_r}{d_r} & \mu \\ 0 & -\Upsilon - d_r - \gamma & 0 & \frac{\delta N b_r}{d_r} & 0 \\ 0 & \gamma & -\Upsilon - \beta - d_r - \omega & 0 & 0 \\ 0 & 0 & \beta & -\Upsilon - d_r - p - q & 0 \\ 0 & 0 & 0 & p & -\Upsilon - d_r - \mu \end{vmatrix}. \tag{4.8}$$

The corresponding eigenvalues are

$$\begin{aligned} \Upsilon_1 &= -0.00082101, \\ \Upsilon_2 &= -0.00060101, \\ \Upsilon_3 &= 0.0318292, \end{aligned}$$

$$\begin{aligned}\Upsilon_4 &= -0.114771,\\ \Upsilon_5 &= -0.284101.\end{aligned}$$

Since one of the eigenvalues is positive, this DFE is unstable. This suggests that the infection can invade and spread.

Similarly, the corresponding eigenvalues of EE point are computed as:

$$\begin{aligned}\Upsilon_1 &= -0.00060101,\\ \Upsilon_2 &= -0.0020132 + 0.0056211i,\\ \Upsilon_3 &= -0.0020132 - 0.0056211i,\\ \Upsilon_4 &= -0.0669139,\\ \Upsilon_5 &= -0.300827.\end{aligned}$$

We see that the eigenvalues have negative real parts. This confirms that the EE is locally asymptotically stable. Small perturbations will decay over time, and the system will return to equilibrium. The presence of complex conjugate eigenvalues suggests damped oscillations in the dynamics around the equilibrium.

We describe the positivity of the model as:

$$\begin{cases} {}^{FFCF}D_{\tau}^{\sigma,\varrho}S(\tau) = Nb_r + \omega V + \mu R \geq 0,\\ {}^{FFCF}D_{\tau}^{\sigma,\varrho}E(\tau) = \delta IS \geq 0,\\ {}^{FFCF}D_{\tau}^{\sigma,\varrho}V(\tau) = \gamma E \geq 0,\\ {}^{FFCF}D_{\tau}^{\sigma,\varrho}I(\tau) = \beta V \geq 0,\\ {}^{FFCF}D_{\tau}^{\sigma,\varrho}R(\tau) = (p+q)I \geq 0. \end{cases} \tag{4.9}$$

Theorem 4.1. *Every solution of* (4.9) *is bounded and it exists inside the boundary region as given by*

$$\Lambda = \left\{(S,E,V,I,R) \in \mathbb{R}_+^5 : N = S + E + V + I + R \leq \frac{Nb_r}{d_r}\right\}.$$

Proof. We have

$$N = S + E + V + I + R. \tag{4.10}$$

Applying the differential operator ${}^{FFCF}D_{\tau}^{\sigma,\varrho}$ to both sides, we have

$${}^{FFCF}D_{\tau}^{\sigma,\varrho}N = {}^{FFCF}D_{\tau}^{\sigma,\varrho}S + {}^{FFCF}D_{\tau}^{\sigma,\varrho}E + {}^{FFCF}D_{\tau}^{\sigma,\varrho}V + {}^{FFCF}D_{\tau}^{\sigma,\varrho}I + {}^{FFCF}D_{\tau}^{\sigma,\varrho}R. \tag{4.11}$$

Using the corresponding values, we have

$${}^{FFCF}D_{\tau}^{\sigma,\varrho}N = Nb_r - Nd_r. \tag{4.12}$$

Taking the limit $\theta \to 0$, and applying Laplace transform, we have

$$N \leq \frac{Nb_r}{d_r}. \tag{4.13}$$

□

5. Existence and stability of the proposed model

Due to the presence of the FFCF derivative in the proposed model, which incorporates both memory effects and nonlocal characteristics through its non-singular kernel, traditional approaches for classical differential equations may not be sufficient. These distinctive features require an independent mathematical investigation to guarantee that the model is well-defined and solvable. Therefore, we conduct an analysis of existence, uniqueness, and stability of the solutions by applying fixed point methods within a suitably chosen functional framework.

We divide the section into four subsections. In the first subsection, we rewrite our model in a compacted form and present its integral form. In the second subsection, we investigate existence of at least one solution. In the third subsection, we investigate the uniqueness of solution of the proposed model. In the last subsection, we carry out Hyers-Ulam stability analysis of the proposed model.

To proceed, we define the Banach space and reformulate the model into an equivalent integral form as presented in the Subsection 5.1.

5.1. Functional framework and integral form

Let the interval $[0, T]$ be represented by $\mathbb{I}$ and define the Banach space as:

$$\mathfrak{B} = C(\mathbb{I}, \mathbb{R}^+) \times C(\mathbb{I}, \mathbb{R}^+) \times C(\mathbb{I}, \mathbb{R}^+) \times C(\mathbb{I}, \mathbb{R}^+) \times C(\mathbb{I}, \mathbb{R}^+)$$

equipped with the following norm

$$\|\xi\| = \max\{|S(\tau)| + |E(\tau)| + |V(\tau)| + |I(\tau)| + |R(\tau)|\};$$

$S, E, V, I, R \in \mathfrak{B}$.

Problem (1.3) can be rewritten as the following system:

$$^{FFCF}D_{\tau}^{\sigma,\varrho}\xi(\tau) = \begin{cases} g(\tau, \xi(\tau)), \\ \xi(0) = \xi_0, \quad \tau \in \mathbb{I}, \end{cases} \tag{5.1}$$

where the vector $\xi(\tau) = (S, E, V, I, R)$ denotes the variable with specified initial condition ξ_0 and the variable function g takes the form:

$$g(\tau, \xi(\tau)) = \begin{bmatrix} \xi_1(\tau, S, E, V, I, R) \\ \xi_2(\tau, S, E, V, I, R) \\ \xi_3(\tau, S, E, V, I, R) \\ \xi_4(\tau, S, E, V, I, R) \\ \xi_5(\tau, S, E, V, I, R) \end{bmatrix}, \ \xi(\tau) = \begin{bmatrix} \xi_1 \\ \xi_2 \\ \xi_3 \\ \xi_4 \\ \xi_5 \end{bmatrix} = \begin{bmatrix} Nb_r - \delta IS(\tau) - d_r S(\tau) + \omega V + \mu R \\ \delta IS(\tau) - \gamma E(\tau) - d_r E(\tau) \\ \gamma E(\tau) - \beta V(\tau) - d_r V(\tau) - \omega V \\ \beta V(\tau) - (p + q + d_r) I(\tau) \\ (p + q) I(\tau) - d_r R(\tau) - \mu R \end{bmatrix},$$

and

$$\xi_0 = \begin{bmatrix} S_0 \\ E_0 \\ V_0 \\ I_0 \\ R_0 \end{bmatrix}.$$

Lemma 5.1. *Problem*

$$ {}^{FFCF}D_{\tau}^{\sigma,\varrho}\xi(\tau) = \begin{cases} \varphi(\tau), & 0 < \sigma, \varrho \leq 1, \text{ if } \tau \in [0,T], \\ & \xi(0) = \xi_0, \end{cases} \tag{5.2} $$

has the solution

$$ \xi(\tau) = \xi_0 + \frac{\varrho(1-\sigma)\tau^{\varrho-1}\varphi(\tau)}{M(\sigma)} + \frac{\sigma\varrho}{M(\sigma)}\int_0^{\tau} y^{\sigma-1}\varphi(y)dy, \quad \tau \in \mathbb{I}. \tag{5.3} $$

Corollary 5.1. *By Lemma 5.1, the solution to the problem* (5.1) *of the proposed model can be expressed as*

$$ \xi(\tau) = \xi_0 + \frac{\varrho(1-\sigma)\tau^{\varrho-1}g(\tau,\xi(\tau))}{M(\sigma)} + \frac{\sigma\varrho}{M(\sigma)}\int_0^{\tau} y^{\sigma-1}g(y,\xi(y))dy, \quad \tau \in \mathbb{I}. \tag{5.4} $$

We introduce the operator $W : \mathfrak{B} \to \mathfrak{B}$ by

$$ W(\xi) = \xi_0 + \frac{\varrho(1-\sigma)\tau^{\varrho-1}g(\tau,\xi(\tau))}{M(\sigma)} + \frac{\sigma\varrho}{M(\sigma)}\int_0^{\tau} y^{\sigma-1}g(y,\xi(y))dy, \quad \tau \in \mathbb{I}. \tag{5.5} $$

For carrying out the coming results, we need to take the following necessary assumptions:

(A_1) Let there exist some constants say $L_g > 0$ such that for $\xi, \overline{\xi} \in \mathfrak{B}$, we have

$$ |g(\tau,\xi(\tau)) - g(\tau,\overline{\xi}(\tau))| \leq L_g|\xi - \overline{\xi}|; $$

(A_2) Assume that there exist constants C_g, and $M_g > 0$ such that

$$ |g(\tau,\xi(\tau))| \leq C_g|\xi(\tau)| + M_g. $$

In the next subsection, we investigate existence of solution of the proposed model.

5.2. Existence of solutions

In this subsection, we investigate the existence of at least one solution of the proposed problem. For investigating this result, we use Krasnoselskii's fixed point theorem.

Theorem 5.1. *If assumptions* $(A_1) - (A_2)$ *hold, then problem* (5.1) *has at least one solution.*

Proof. We change (5.1) into a fixed point problem by

$$ \xi = W(\xi(\tau)), \quad \xi \in \mathfrak{B}. $$

We consider a close ball $\Omega_\theta = \{\xi \in \mathfrak{B} : \|\xi\| \leq \theta\}$ with

$$ \theta \geq \frac{|\xi_0| + \frac{M_g\varrho}{M(\sigma)}\left((1-\sigma)T^{\varrho-1} + T^{\sigma}\right)}{1 - \frac{C_g\varrho}{M(\sigma)}\left((1-\sigma)T^{\varrho-1} + T^{\sigma}\right)}. $$

We take the operator W as sum of the two sub-operators W_1 and W_2 such that

$$ W_1\xi(\tau) = \Big\{\xi_0 + \frac{\varrho(1-\sigma)\tau^{\varrho-1}g(\tau,\xi(\tau))}{M(\sigma)}, \tag{5.6} $$

and

$$W_2\xi(\tau) = \left\{\frac{\sigma\varrho}{M(\sigma)}\int_0^\tau y^{\sigma-1}g(y,\xi(y))dy. \right. \tag{5.7}$$

Several steps are involved in accomplishing the proof.

Step 1: $W_1\xi(\tau) + W_2\xi(\tau) \in \Omega_\theta$. For $\tau \in \mathbb{I}$, $\xi \in \Omega_\theta$, with (A_2), we have

$$\begin{aligned}
&|W_1\xi(\tau) + W_2\xi(\tau)| = \left|\xi(\tau_0) + \frac{\varrho(1-\sigma)\tau^{\varrho-1}g(\tau,\xi(\tau))}{M(\sigma)} + \frac{\sigma\varrho}{M(\sigma)}\int_0^\tau y^{\sigma-1}g(y,\xi(y))dy\right| \\
&\leq |\xi_0| + \frac{\varrho(1-\sigma)\tau^{\varrho-1}\,|g(\tau,\xi(\tau))|}{M(\sigma)} + \frac{\sigma\varrho}{M(\sigma)}\int_0^\tau y^{\sigma-1}\,|g(y,\xi(y))|\,dy \\
&\leq |\xi_0| + \frac{M_g\varrho}{M(\sigma)}\Big((1-\sigma)T^{\varrho-1} + T^\sigma\Big) + \frac{C_g\varrho}{M(\sigma)}\Big((1-\sigma)T^{\varrho-1} + T^\sigma\Big)\theta \leq \theta.
\end{aligned} \tag{5.8}$$

Hence, $W_1\xi(\tau) + W_2\xi(\tau) \in \Omega_\theta$.

Step 2: W_1 is a contraction.

For $\tau \in \mathbb{I}$, $\xi_1, \xi_2 \in \Omega_\theta$. Then,

$$\begin{aligned}
&|W_1\xi_1(\tau) - W_1\xi_2(\tau)| = \max_{\tau\in[0,T]}\left(|\xi_1(\tau_1) - \xi_2(\tau_1)| + \frac{\varrho(1-\sigma)\tau^{\varrho-1}}{M(\sigma)}\,|g(\tau,\xi_1(\tau)) - g(\tau,\xi_2(\tau))|\right) \\
&\leq\left(1 + \frac{\varrho(1-\sigma)T^{\varrho-1}L_g}{M(\sigma)}\right)\|\xi_1 - \xi_2\|;
\end{aligned} \tag{5.9}$$

if $1 + \frac{\varrho(1-\sigma)T^{\varrho-1}L_g}{M(\sigma)} \leq 1$, then W_1 is a contraction.

Step 3: In this step, we will show the relative compactness of W_2. Consequently, we will show that W_2 is continuous, uniformly bounded on Ω_θ, and equi-continuous.

W_2 is continuous due to the continuity of $g(\tau,\xi(\tau))$.

W_2 is uniformly bounded on Ω_θ:

For $\tau \in \mathbb{I}$, $\xi \in \Omega_\theta$, we consider

$$\begin{aligned}
|W_2\xi(\tau)| &= \frac{\sigma\varrho}{M(\sigma)}\int_0^\tau y^{\sigma-1}\,|g(y,\xi(y))|\,dy \\
&\leq\Big(C_g|\theta| + M_g\Big)\frac{\varrho}{M(\sigma)}T^\sigma \leq \theta.
\end{aligned} \tag{5.10}$$

Thus W_2 is uniformly bounded on Ω_θ.

Next, we need to establish equi-continuity.

Let $\tau_a, \tau_b \in \mathbb{I}$ with $\tau_a < \tau_b$. Then

$$\begin{aligned}
\|W_2\xi(\tau_b) - W_2\xi(\tau_a)\| &\leq \frac{\sigma\varrho}{M(\sigma)}\int_0^{\tau_b} y^{\varrho-1}\,|g(y,\xi(y))|\,dy - \frac{\sigma\varrho}{M(\sigma)}\int_0^{\tau_a} y^{\varrho-1}\,|g(y,\xi(y))|\,dy \\
&\leq \frac{\sigma\varrho}{M(\sigma)}\Big(\int_0^{\tau_b} y^{\varrho-1}\,|g(y,\xi(y))|\,dy - \int_0^{\tau_a} y^{\varrho-1}\,|g(y,\xi(y))|\,dy\Big) \\
&= \frac{\sigma}{M(\sigma)}\Big((\tau_b)^\varrho - (\tau_a)^\varrho\Big)\Big(C_g\theta + M_g\Big) \\
&\to 0 \text{ as } \tau_b \to \tau_a.
\end{aligned}$$

This proves that W_2 is equi-continuous. Thus, W is relatively compact via the Arzelá-Ascoli theorem and the above steps, and its complete continuity is ensured. It follows that, by Theorem 2.1, there is at least one solution for problem (5.1). □

The next subsection is allocated for investigation of uniqueness of solution.

5.3. Uniqueness of solutions

In this subsection, we use Banach's fixed point theorem to derive conditions for uniqueness of solution of the proposed model.

Theorem 5.2. *Under assumption* (A_1) *and the condition* $\frac{L_g}{M(\sigma)}\left(\varrho\,(1-\sigma)\,T^{\varrho-1}+\sigma T^{\varrho}\right)<1$, *problem of model* (5.1) *has a unique solution.*

Proof. For $\tau\in\mathbb{I}$, $\xi_1,\xi_2\in\Omega_\theta$. We have

$$\begin{aligned}|W\xi_1(\tau)-W\xi_2(\tau)| &\leq \max_{\tau\in\mathbb{I}}\Big[\frac{(1-\sigma)}{M(\sigma)}\varrho\tau^{\varrho-1}\,|g(\tau,\xi_1(\tau))-g(\tau,\xi_2(\tau))|\\ &\quad+\frac{\sigma\varrho}{\mathbb{M}(\sigma)}\int_0^{\tau}y^{\varrho-1}\,|g(y,\xi_1(y))-g(y,\xi_2(y))|\,dy\Big]\\ &\leq \max_{\tau\in\mathbb{I}}\Big[\frac{(1-\sigma)L_g}{M(\sigma)}\varrho\tau^{\varrho-1}\,|\xi_1(\tau)-\xi_2(\tau)|\\ &\quad+\frac{\sigma L_g T^{\varrho}}{M(\sigma)}\,|\xi_1(\tau)-\xi_2(\tau)|\Big].\end{aligned}$$

Hence

$$\|W\xi_1-W\xi_2\|\leq\frac{L_g}{M(\sigma)}\left(\varrho\,(1-\sigma)\,T^{\varrho-1}+\sigma T^{\varrho}\right)\|\xi_1-\xi_2\|.$$

Since $\frac{L_g}{M(\sigma)}\left(\varrho\,(1-\sigma)\,T^{\varrho-1}+\sigma T^{\varrho}\right)<1$, it follows that W is a contraction, and, therefore, the solution of model (5.1) is unique. □

In the coming subsection, we carry out stability analysis of the proposed model.

5.4. Stability analysis

Definition 5.1. The model prescribed by (5.1) is H-U stable if there is a real number $\mathbf{c}>0\ni$ for each $\epsilon>0$, any solution $\widehat{\xi}\in\mathfrak{B}$ of inequality is

$$\left|{}^{PFFCF}D_{\tau}^{\sigma,\varrho}\widehat{\xi}(\tau)-g(\tau,\widehat{\xi}(\tau))\right|\leq\epsilon,\tau\in\mathbb{I},$$

and unique solution $\xi\in\mathfrak{B}$ of model (5.1) in the following inequality satisfies

$$\left\|\widehat{\xi}-\xi\right\|\leq\mathbf{c}\epsilon,\qquad\tau\in\mathbb{I},$$

where

$$\widehat{\xi}(\tau)=\begin{pmatrix}\widehat{S}(\tau)\\ \widehat{E}(\tau)\\ \widehat{V}(\tau)\\ \widehat{I}(\tau)\\ \widehat{R}(\tau)\end{pmatrix},\widehat{\xi}(0)=\begin{pmatrix}\widehat{S}(0)\\ \widehat{E}(0)\\ \widehat{V}(0)\\ \widehat{I}(0)\\ \widehat{R}(0)\end{pmatrix},g(\tau,\widehat{\xi}(\tau))=\begin{pmatrix}\widehat{\xi}_1(\tau,\widehat{S},\widehat{E},\widehat{V},\widehat{I},\widehat{R})\\ \widehat{\xi}_2(\tau,\widehat{S},\widehat{E},\widehat{V},\widehat{I},\widehat{R})\\ \widehat{\xi}_3(\tau,\widehat{S},\widehat{E},\widehat{V},\widehat{I},\widehat{R})\\ \widehat{\xi}_4(\tau,\widehat{S},\widehat{E},\widehat{V},\widehat{I},\widehat{R})\\ \widehat{\xi}_5(\tau,\widehat{S},\widehat{E},\widehat{V},\widehat{I},\widehat{R})\end{pmatrix}.$$

Remark 5.1. Let there be a small perturbation $\Psi \in \mathfrak{B}$ such that

(i) $|\Psi(\tau)| \leq \epsilon,\ \tau \in \mathbb{I}$;

(ii) ${}^{PFFCF}D_{\tau}^{\sigma,\varrho}\widehat{\xi}(\tau) = g(\tau, \widehat{\xi}(\tau)) + \Psi(\tau),\ \tau \in \mathbb{I}$.

A perturbed problem solution is derived by Remark 5.1,

$$\begin{cases} {}^{PFFCF}D_{\tau}^{\sigma,\varrho}\widehat{\xi}(\tau) = g(\tau, \widehat{\xi}(\tau)) + \Psi(\tau), \\ \widehat{\xi}(0) = \widehat{\xi}_0 > 0. \end{cases} \tag{5.11}$$

Lemma 5.2. *The solution of problem* (5.11) *that has a perturbation function* $\Psi(\tau)$ *is provided by*

$$\widehat{\xi}(\tau) = \widehat{\xi}_0 + \frac{\varrho(1-\sigma)\tau^{\varrho-1}(g(\tau, \widehat{\xi}(\tau)) + \Psi(\tau))}{M(\sigma)} + \frac{\sigma\varrho}{M(\sigma)}\int_0^{\tau} y^{\sigma-1}(g(y, \widehat{\xi}(y)) + \Psi(y))dy, \quad \tau \in \mathbb{I}. \tag{5.12}$$

Proof. The proof can be obtained by using Lemma 5.1. □

Theorem 5.3. *Under assumption* (A_1) *and the condition* $\frac{L_g}{M(\sigma)}\left(\varrho\,(1-\sigma)\,T^{\varrho-1} + \sigma T^{\varrho}\right) < 1$, *model* (5.1) *is H-U stable.*

Proof. Let $\xi, \widehat{\xi} \in \mathfrak{B}$ be the unique and any solution of model (5.1) and (5.11), respectively. For $\tau \in (\tau_1, T]$, using (5.4) and (5.12), we have

$$\begin{aligned} &\left|\widehat{\xi}(\tau) - \xi(\tau)\right| \leq \frac{\varrho(1-\sigma)\tau^{\varrho-1}}{M(\sigma)}\left|g(\tau, \widehat{\xi}(\tau)) - g(\tau, \xi(\tau))\right| + \frac{\sigma\varrho}{M(\sigma)}\int_0^{\tau} y^{\sigma-1}\left|g(\tau, \widehat{\xi}(\tau)) - g(\tau, \xi(\tau))\right| dy \\ &+ \frac{\varrho(1-\sigma)\tau^{\varrho-1}}{M(\sigma)}\left|\Psi(\tau)\right| + \frac{\sigma\varrho}{M(\sigma)}\int_0^{\tau} y^{\sigma-1}\left|\Psi(\tau)\right| dy \\ \leq &\frac{L_g}{M(\sigma)}\left(\varrho\,(1-\sigma)\,T^{\varrho-1} + \sigma T^{\varrho}\right)\left\|\widehat{\xi} - \xi\right\| + \left(\frac{\varrho(1-\sigma)T^{\varrho-1}}{M(\sigma)} + \frac{\varrho}{M(\sigma)}T^{\sigma}\right)\epsilon. \end{aligned} \tag{5.13}$$

Further simplification implies

$$\left\|\widehat{\xi} - \xi\right\| \leq \frac{\left(\frac{\varrho(1-\sigma)T^{\varrho-1}}{M(\sigma)} + \frac{\varrho}{M(\sigma)}T^{\sigma}\right)}{1 - \left(\frac{L_g}{M(\sigma)}\left(\varrho\,(1-\sigma)\,T^{\varrho-1} + \sigma T^{\varrho}\right)\right)}\epsilon. \tag{5.14}$$

This implies that

$$\left\|\widehat{\xi} - \xi\right\| \leq \mathbf{c}\epsilon,$$

where

$$\mathbf{c} = \frac{\left(\frac{\varrho(1-\sigma)T^{\varrho-1}}{M(\sigma)} + \frac{\varrho}{M(\sigma)}T^{\sigma}\right)}{1 - \left(\frac{L_g}{M(\sigma)}\left(\varrho\,(1-\sigma)\,T^{\varrho-1} + \sigma T^{\varrho}\right)\right)}. \tag{5.15}$$

This proves that model (5.1) is H-U stable. □

6. Simulation-based solution of (1.3)

In this section, we aim to find a numerical solution for model (5.1) under FFCF derivative. To develop the numerical scheme for the proposed model, we use the extended 2-step Adams-Bashforth method (ABM) with Lagrange interpolation as used in [33]. The corresponding integral form of the model, at $\tau = \tau_{a+1}$, is presented as

$$\begin{cases} S^{a+1} = S(0) + \dfrac{\varrho(1-\sigma)\tau_a^{\varrho-1}\xi_1(\tau_a,S,E,V,I,R)}{M(\sigma)} + \dfrac{\sigma\varrho}{M(\sigma)}\displaystyle\int_0^{\tau_a} y^{\sigma-1}\xi_1(y,S,E,V,I,R)dy, \quad \tau_a \in \mathbb{I}, \\ E^{a+1} = E(0) + \dfrac{\varrho(1-\sigma)\tau_a^{\varrho-1}\xi_2(\tau_a,S,E,V,I,R)}{M(\sigma)} + \dfrac{\sigma\varrho}{M(\sigma)}\displaystyle\int_0^{\tau_a} y^{\sigma-1}\xi_2(y,S,E,V,I,R)dy, \quad \tau_a \in \mathbb{I}, \\ V^{a+1} = V(0) + \dfrac{\varrho(1-\sigma)\tau_a^{\varrho-1}\xi_3(\tau_a,S,E,V,I,R)}{M(\sigma)} + \dfrac{\sigma\varrho}{M(\sigma)}\displaystyle\int_0^{\tau_a} y^{\sigma-1}\xi_3(y,S,E,V,I,R)dy, \quad \tau_a \in \mathbb{I}, \\ I^{a+1} = I(0) + \dfrac{\varrho(1-\sigma)\tau_a^{\varrho-1}\xi_4(\tau_a,S,E,V,I,R)}{M(\sigma)} + \dfrac{\sigma\varrho}{M(\sigma)}\displaystyle\int_0^{\tau_a} y^{\sigma-1}\xi_4(y,S,E,V,I,R)dy, \quad \tau_a \in \mathbb{I}, \\ R^{a+1} = R(0) + \dfrac{\varrho(1-\sigma)\tau_a^{\varrho-1}\xi_5(\tau_a,S,E,V,I,R)}{M(\sigma)} + \dfrac{\sigma\varrho}{M(\sigma)}\displaystyle\int_0^{\tau_a} y^{\sigma-1}\xi_5(y,S,E,V,I,R)dy, \quad \tau_a \in \mathbb{I}. \end{cases} \tag{6.1}$$

We then approximate the systems as

$$\begin{cases} S^{a+1} = \begin{cases} S(0) + \frac{\varrho(1-\sigma)\tau_a^{\varrho-1}\xi_1(\tau_a,S^a,E^a,V^a,I^a,R^a)}{M(\sigma)} - \frac{\varrho(1-\sigma)\tau_{a-1}^{\varrho-1}\xi_1(\tau_{a-1},S^{a-1},E^{a-1},I^{a-1},R^{a-1})}{M(\sigma)} \\ \quad + \frac{\sigma\varrho}{M(\sigma)}\int_{\tau_a}^{\tau_{a+1}} y^{\sigma-1}\xi_1(y,S,E,V,I,R)dy, \quad \tau_a,\tau_{a+1} \in \mathbb{I}, \end{cases} \\ E^{a+1} = \begin{cases} E(0) + \frac{\varrho(1-\sigma)\tau_a^{\varrho-1}\xi_2(\tau_a,S^a,E^a,V^a,I^a,R^a)}{M(\sigma)} - \frac{\varrho(1-\sigma)\tau_{a-1}^{\varrho-1}\xi_2(\tau_{a-1},S^{a-1},E^{a-1},I^{a-1},R^{a-1})}{M(\sigma)} \\ \quad + \frac{\sigma\varrho}{M(\sigma)}\int_{\tau_a}^{\tau_{a+1}} y^{\sigma-1}\xi_2(y,S,E,V,I,R)dy, \quad \tau_a,\tau_{a+1} \in \mathbb{I}, \end{cases} \\ V^{a+1} = \begin{cases} V(0) + \frac{\varrho(1-\sigma)\tau_a^{\varrho-1}\xi_3(\tau_a,S^a,E^a,V^a,I^a,R^a)}{M(\sigma)} - \frac{\varrho(1-\sigma)\tau_{a-1}^{\varrho-1}\xi_3(\tau_{a-1},S^{a-1},E^{a-1},I^{a-1},R^{a-1})}{M(\sigma)} \\ \quad + \frac{\sigma\varrho}{M(\sigma)}\int_{\tau_a}^{\tau_{a+1}} y^{\sigma-1}\xi_3(y,S,E,V,I,R)dy, \quad \tau_a,\tau_{a+1} \in \mathbb{I}, \end{cases} \\ I^{a+1} = \begin{cases} I(0) + \frac{\varrho(1-\sigma)\tau_a^{\varrho-1}\xi_4(\tau_a,S^a,E^a,V^a,I^a,R^a)}{M(\sigma)} - \frac{\varrho(1-\sigma)\tau_{a-1}^{\varrho-1}\xi_4(\tau_{a-1},S^{a-1},E^{a-1},I^{a-1},R^{a-1})}{M(\sigma)} \\ \quad + \frac{\sigma\varrho}{M(\sigma)}\int_{\tau_a}^{\tau_{a+1}} y^{\sigma-1}\xi_4(y,S,E,V,I,R)dy, \quad \tau_a,\tau_{a+1} \in \mathbb{I}, \end{cases} \\ R^{a+1} = \begin{cases} R(0) + \frac{\varrho(1-\sigma)\tau_a^{\varrho-1}\xi_5(\tau_a,S^a,E^a,V^a,I^a,R^a)}{M(\sigma)} - \frac{\varrho(1-\sigma)\tau_{a-1}^{\varrho-1}\xi_5(\tau_{a-1},S^{a-1},E^{a-1},I^{a-1},R^{a-1})}{M(\sigma)} \\ \quad + \frac{\sigma\varrho}{M(\sigma)}\int_{\tau_a}^{\tau_{a+1}} y^{\sigma-1}\xi_5(y,S,E,V,I,R)dy, \quad \tau_a,\tau_{a+1} \in \mathbb{I}. \end{cases} \end{cases} \tag{6.2}$$

For approximation of the integrals, we employ Lagrange interpolation, and obtain the following numerical solution:

$$
\begin{cases}
S^{a+1} = \begin{cases} S(0) + \frac{\varrho(1-\sigma)\tau_a^{\varrho-1}\xi_1(\tau_a,S^a,E^a,V^a,I^a,R^a)}{M(\sigma)} - \frac{\varrho(1-\sigma)\tau_{a-1}^{\varrho-1}\xi_1(\tau_{a-1},S^{a-1},E^{a-1},I^{a-1},R^{a-1})}{M(\sigma)} \\ +\frac{\varrho\sigma}{M(\sigma)}\frac{3}{2}(\Delta\tau)\tau_a^{\varrho-1}\xi_1(\tau_a,S^a,E^a,V^a,I^a,R^a) - \frac{\varrho\sigma}{M(\sigma)}\frac{(\Delta\tau)}{2}\tau_{a-1}^{\varrho-1}\xi_1(\tau_{a-1},S^{a-1},E^{a-1},I^{a-1},R^{a-1}), \\ \tau_a,\tau_{a-1}\in\mathbb{I}, \end{cases} \\
E^{a+1} = \begin{cases} E(0) + \frac{\varrho(1-\sigma)\tau_a^{\varrho-1}\xi_2(\tau_a,S^a,E^a,V^a,I^a,R^a)}{M(\sigma)} - \frac{\varrho(1-\sigma)\tau_{a-1}^{\varrho-1}\xi_2(\tau_{a-1},S^{a-1},E^{a-1},I^{a-1},R^{a-1})}{M(\sigma)} \\ +\frac{\varrho\sigma}{M(\sigma)}\frac{3}{2}(\Delta\tau)\tau_a^{\varrho-1}\xi_2(\tau_a,S^a,E^a,V^a,I^a,R^a) - \frac{\varrho\sigma}{M(\sigma)}\frac{(\Delta\tau)}{2}\tau_{a-1}^{\varrho-1}\xi_2(\tau_{a-1},S^{a-1},E^{a-1},I^{a-1},R^{a-1}), \\ \tau_a,\tau_{a-1}\in\mathbb{I}, \end{cases} \\
V^{a+1} = \begin{cases} V(0) + \frac{\varrho(1-\sigma)\tau_a^{\varrho-1}\xi_3(\tau_a,S^a,E^a,V^a,I^a,R^a)}{M(\sigma)} - \frac{\varrho(1-\sigma)\tau_{a-1}^{\varrho-1}\xi_3(\tau_{a-1},S^{a-1},E^{a-1},I^{a-1},R^{a-1})}{M(\sigma)} \\ +\frac{\varrho\sigma}{M(\sigma)}\frac{3}{2}(\Delta\tau)\tau_a^{\varrho-1}\xi_3(\tau_a,S^a,E^a,V^a,I^a,R^a) - \frac{\varrho\sigma}{M(\sigma)}\frac{(\Delta\tau)}{2}\tau_{a-1}^{\varrho-1}\xi_3(\tau_{a-1},S^{a-1},E^{a-1},I^{a-1},R^{a-1}), \\ \tau_a,\tau_{a-1}\in\mathbb{I}, \end{cases} \\
I^{a+1} = \begin{cases} I(0) + \frac{\varrho(1-\sigma)\tau_a^{\varrho-1}\xi_4(\tau_a,S^a,E^a,V^a,I^a,R^a)}{M(\sigma)} - \frac{\varrho(1-\sigma)\tau_{a-1}^{\varrho-1}\xi_4(\tau_{a-1},S^{a-1},E^{a-1},I^{a-1},R^{a-1})}{M(\sigma)} \\ +\frac{\varrho\sigma}{M(\sigma)}\frac{3}{2}(\Delta\tau)\tau_a^{\varrho-1}\xi_4(\tau_a,S^a,E^a,V^a,I^a,R^a) - \frac{\varrho\sigma}{M(\sigma)}\frac{(\Delta\tau)}{2}\tau_{a-1}^{\varrho-1}\xi_4(\tau_{a-1},S^{a-1},E^{a-1},I^{a-1},R^{a-1}), \\ \tau_a,\tau_{a-1}\in\mathbb{I}, \end{cases} \\
R^{a+1} = \begin{cases} R(0) + \frac{\varrho(1-\sigma)\tau_a^{\varrho-1}\xi_5(\tau_a,S^a,E^a,V^a,I^a,R^a)}{M(\sigma)} - \frac{\varrho(1-\sigma)\tau_{a-1}^{\varrho-1}\xi_5(\tau_{a-1},S^{a-1},E^{a-1},I^{a-1},R^{a-1})}{M(\sigma)} \\ +\frac{\varrho\sigma}{M(\sigma)}\frac{3}{2}(\Delta\tau)\tau_a^{\varrho-1}\xi_5(\tau_a,S^a,E^a,V^a,I^a,R^a) - \frac{\varrho\sigma}{M(\sigma)}\frac{(\Delta\tau)}{2}\tau_{a-1}^{\varrho-1}\xi_5(\tau_{a-1},S^{a-1},E^{a-1},I^{a-1},R^{a-1}), \\ \tau_a,\tau_{a-1}\in\mathbb{I}. \end{cases}
\end{cases} \tag{6.3}
$$

7. Simulations and analysis

In this section, using the parameters values in Table 1, we simulate numerical results of the proposed SEVIR-S model. In the first two figures, we give two comparative plots of the model via the 2-step ABM and Euler method. A numerical sanity check is carried out to ensure that the ABM numerical method is well behaved at least for the case of $\sigma = \rho = 1$.

In Figures 1 and 2, we observe that for fractional order $\sigma = 1$, and fractal dimension $\varrho = 1$, the ABM method gives identical dynamical behavior to that by the Euler method. Hence, ABM method is well behaved at least for the case of $\sigma = \rho = 1$.

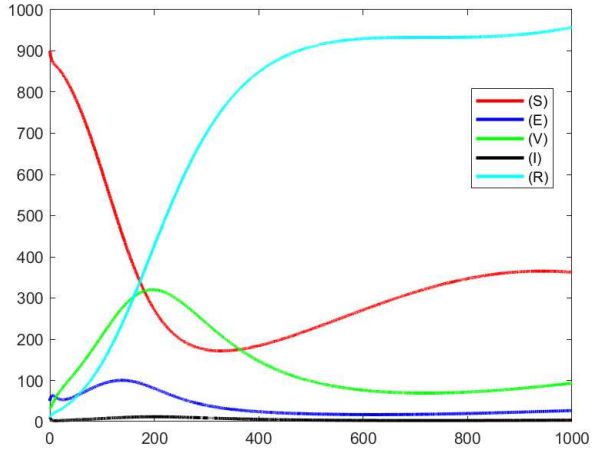

Figure 1. Dynamical behavior of model (1.3) via proposed ABM method for $\sigma = 1, \varrho = 1$.

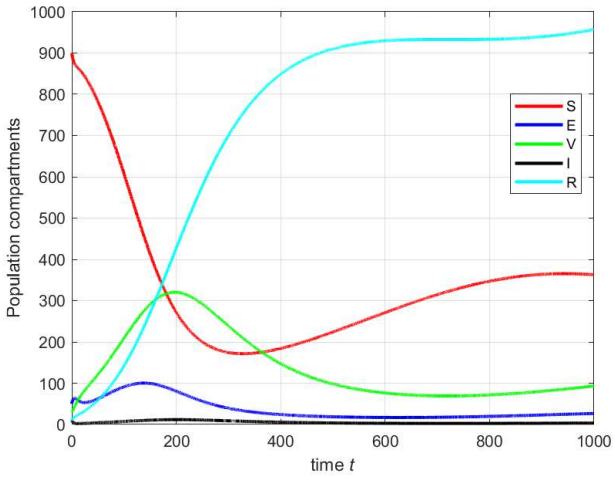

Figure 2. Classical SEVIR-S model using Euler method.

Next, using the two steps ABM numerical method, we simulate the numerical results under fractional-order and fractal-dimensional variations to observe the dynamics of different compartments of the proposed SEVIR-S model. In the Figures 3–7, the fractal dimension is kept constant while the fractional order is being changed to see the impact of fractional order on the model's dynamics. Similarly in the Figures 8–12, the fractional order is kept constant while the fractal dimension is being changed to see the impact of fractal dimension on the model's dynamics.

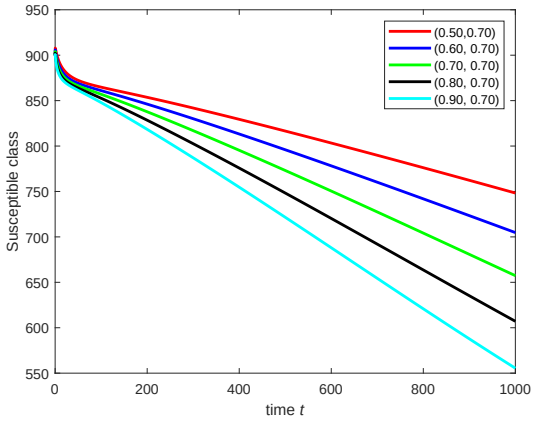

Figure 3. Dynamical behavior of susceptible class on various fractional orders with same fractal dimension.

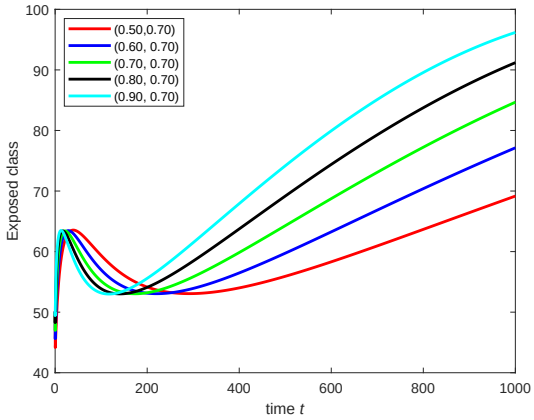

Figure 4. Dynamical behavior of exposed class on various fractional orders with same fractal dimension.

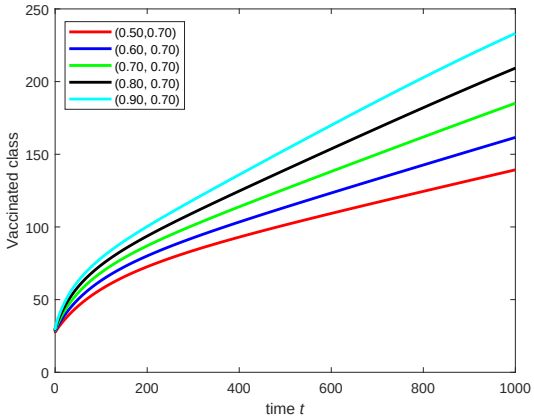

Figure 5. Dynamical behavior of vaccinated class on various fractional orders with same fractal dimension.

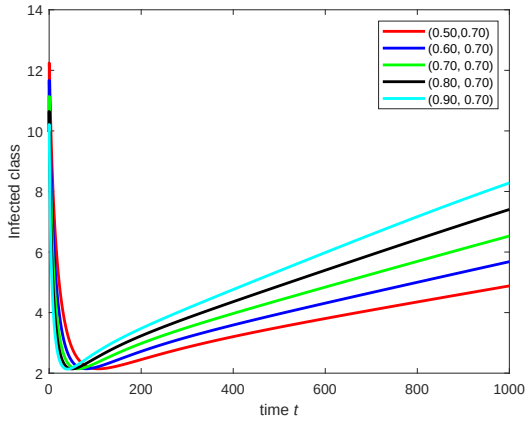

Figure 6. Dynamical behavior of infected class on various fractional orders with same fractal dimension.

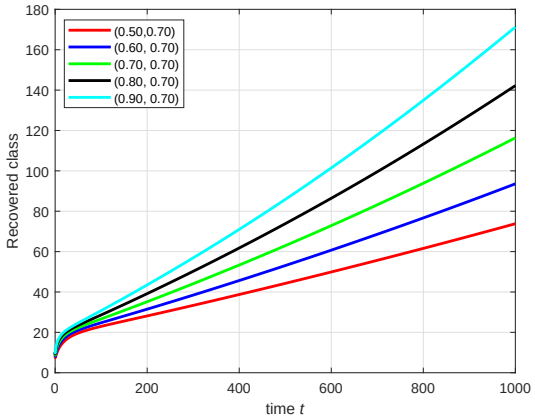

Figure 7. Dynamical behavior of recovered class on various fractional orders with same fractal dimension.

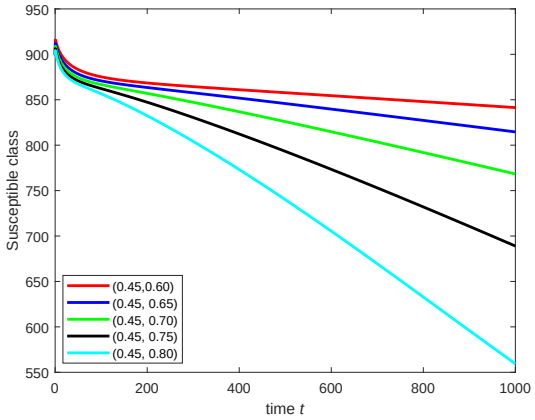

Figure 8. Dynamical behavior of susceptible class on various fractal dimensions with fixed fractional orders.

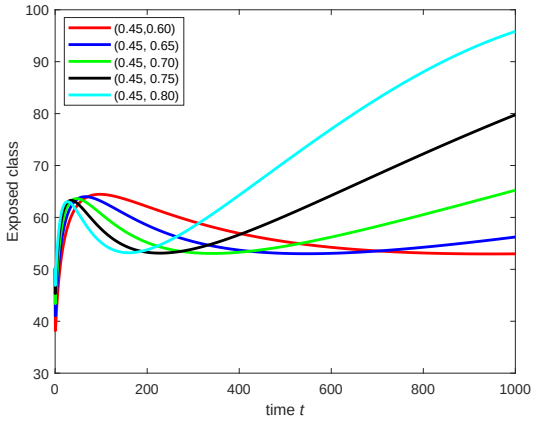

Figure 9. Dynamical behavior of exposed class on various fractal dimensions with fixed fractional orders.

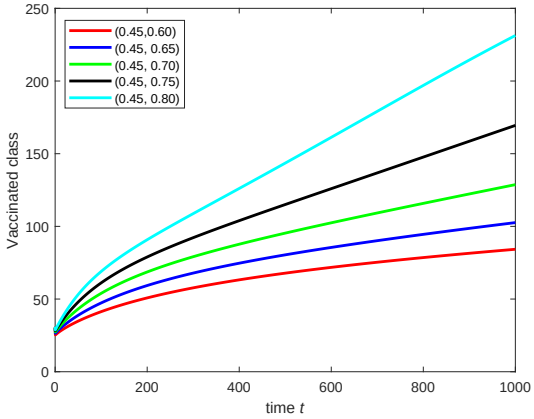

Figure 10. Dynamical behavior of vaccinated class on various fractal dimensions with fixed fractional orders.

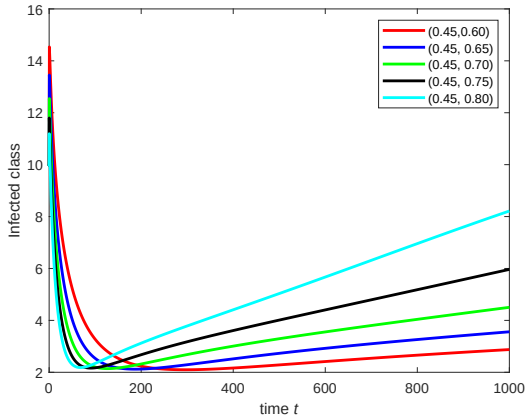

Figure 11. Dynamical behavior of infected class on various fractal dimensions with fixed fractional orders.

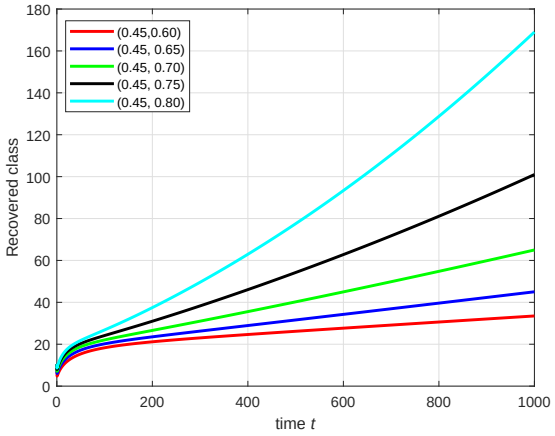

Figure 12. Dynamical behavior of recovered class on various fractal dimensions with fixed fractional orders.

For simulation, we utilized MATLAB R2024a on a system equipped with an Intel(R) Core(TM) i5-8350U CPU @ 1.70GHz 1.90GHz, RAM 16 GB. With a step size $h = 0.05$ and final time simulation time $t = 1000$, the average CPU time for the proposed ABM numerical method computed over multiple simulation runs and was approximately 1.45 seconds per figure.

The following analysis offers deeper insight into the behavior of the SEVIR-S model as depicted in Figures 3–12.

Figures 3–7 depict the dynamical behavior of each compartment (susceptible, exposed, vaccinated, infected, and recovered) under varying fractional orders while keeping the fractal dimension fixed at 0.70. As the fractional order increases, the solution becomes more regular and stabilizes faster. Lower fractional orders correspond to systems with stronger memory effects, showing delayed convergence or oscillatory dynamics. This highlights the sensitivity of the model to memory effects encoded by the fractional parameter σ.

Figures 8–12 demonstrate the effect of changing fractal dimension values while keeping the fractional order fixed. The fractal dimension captures structural irregularities and heterogeneity in population behavior. As the dimension increases, the dynamics generally reflect greater complexity and higher peaks, especially in the exposed and infected compartments. This illustrates that more intricate population structures may lead to stronger epidemic waves.

Across all figures, we observe that the interplay between fractional order and fractal dimension allows fine control over the dynamics. Such sensitivity analysis is essential for fitting real-world data and capturing diverse epidemic patterns. The vaccinated class shows significant responsiveness to both parameters, indicating its critical role in shaping epidemic control strategies.

8. Conclusions

In this study, we proposed an extended SEVIR-S model for the spread of adenovirus by incorporating immunity waning and reinfection-key aspects often overlooked in classical models. This modification allows for a more realistic representation of diseases like adenovirus, where recovered individuals may lose immunity and become susceptible again. The model was developed using the

FFCF derivative with a power-law kernel, enabling a more accurate description of memory effects and complex dynamics. We derived and analyzed equilibrium points corresponding to disease-free and endemic states. Also, we calculated R_0, which is essential for understanding the long-term behavior of the disease. The existence of solutions was established through the fixed point approach, and the model's stability was rigorously examined using the Hyers-Ulam Stability technique. Numerical simulations, carried out using an extended second-order ABM, validated our theoretical findings and demonstrated the dynamic behavior of the model under different parameter settings. Including reinfection and immunity waning in our model makes it much more realistic-especially for diseases like adenovirus, COVID-19, or influenza where immunity isn't lifelong. It captures the possibility of endemicity and the need for booster doses. Overall, the proposed model offers a well-defined framework for analyzing the transmission dynamics of adenovirus, capturing the influence of reinfection and immunity waning, and can be extended to other infectious diseases with similar characteristics.

Author contributions

Rabeb Sidaoui: Methodology, formal analysis, investigation; W. Eltayeb Ahmed: Methodology, formal analysis, investigation; Arshad Ali: Conceptualization, writing—original draft; Mohammed Rabih: Writing—review & editing; Amer Alsulami: Writing—review & editing; Khaled Aldwoah: Writing—review & editing, supervision, project administration; E. I. Hassan: Methodology, formal analysis. All authors have read and agreed to the published version of the manuscript.

Use of Generative-AI tools declaration

The authors declare they have not used Artificial Intelligence (AI) tools in the creation of this article.

Data availability

The paper contains all data that was either created or analyzed throughout the course of this research.

Acknowledgments

This work was supported and funded by the Deanship of Scientific Research at Imam Mohammad Ibn Saud Islamic University (IMSIU) (grant number IMSIU-DDRSP2501).

Conflict of interest

The authors declare that they have no conflicts of interest.

References

1. *Conjunctivitis (pink eye)*, Center for Disease Control. Available from: `https://www.cdc.gov/conjunctivitis/index.html`.

2. S. R. Fehily, G. B. Cross, A. J. Fuller, Bilateral conjunctivitis in a returned traveler, *PLoS Negl. Trop. Dis.*, **9** (2015), e0003351. https://doi.org/10.1371/journal.pntd.0003351

3. R. H. Elliot, Conjunctivitis in the tropics, *Br. Med. J.*, **1** (1925), 12. https://doi.org/10.1136/bmj.1.3340.12-a

4. K. N. Malu, Allergic conjunctivitis in Jos-Nigeria, *Niger. Med. J.*, **55** (2014), 166–170. https://doi.org/10.4103/0300-1652.129664

5. AAP Committee on Infectious Diseases, *Red book: 2018-2021 Report of the committee on infectious diseases*, 31st Eds., American Academy of Pediatrics, 2018.

6. S. Sangsawang, T. Tanutpanit, W. Mumtong, P. Pongsumpun, Local stability analysis of mathematical model for hemorrhagic conjunctivitis disease, *Curr. Appl. Sci. Technol.*, **12** (2012), 189–197.

7. O. Ghazali, K. B. Chua, K. P. Ng, P. S. Hooi, M. A. Pallansch, M. S. Oberste, et al., An outbreak of acute haemorrhagic conjunctivitis in Melaka, Malaysia, *Singapore Med. J.*, **44** (2003), 511–516.

8. J. Chansaenroj, S. Vongpunsawad, J. Puenpa, A. Theamboonlers, V. Vuthitanachot, P. Chattakul, et al., Epidemic outbreak of acute haemorrhagic conjunctivitis caused by coxsackievirus A24 in Thailand, 2014, *Epidemiol. Infect.*, **143** (2015), 3087–3093. https://doi.org/10.1017/S0950268815000643

9. G. Chowell, E. Shim, F. Brauer, P. Diaz-Dueas, J. M. Hyman, C. Castillo-Chavez, Modelling the transmission dynamics of acute haemorrhagic conjunctivitis: Application to the 2003 outbreak in Mexico, *Stat. Med.*, **25** (2006), 1840–1857. https://doi.org/10.1002/sim.2352

10. J. Suksawat, S. Naowarat, Effect of rainfall on the transmission model of conjunctivitis, *Adv. Environ. Biol.*, **8** (2014), 99–104.

11. B. Unyong, S. Naowarat, Stability analysis of conjunctivitis model with nonlinear incidence term, *Aust. J. Basic Appl. Sci.*, **8** (2014), 52–58.

12. S. Sangthongjeen, A. Sudchumnong, S. Naowarat, Effect of educational campaign on transmission model of conjunctivitis, *Aust. J. Basic Appl. Sci.*, **9** (2015), 811–815.

13. F. Javed, A. Ahmad, A. H. Ali, E. Hincal, A. Amjad, Investigation of conjunctivitis adenovirus spread in human eyes by using bifurcation tool and numerical treatment approach, *Phys. Scr.*, **99** (2024), 085253. https://doi.org/10.1088/1402-4896/ad62a5

14. K. S. Nisar, A. Ahmad, M. Farman, E. Hincal, A. Zehra, Modeling and mathematical analysis of fractional order eye infection (conjunctivitis) virus model with treatment impact: Prelicence and dynamical transmission, *Alex. Eng. J.*, **107** (2024), 33–46. https://doi.org/10.1016/j.aej.2024.07.020

15. C. S. Chou, A. Friedman, *Introduction to mathematical biology: Modeling, analysis, and simulations*, Cham: Springer, 2016. https://doi.org/10.1007/978-3-319-29638-8

16. E. K. Yeargers, R. W. Shonkwiler, J. V. Herod, *An introduction to the mathematics of biology: With computer algebra models*, Boston: Birkhäuser, 2013. https://doi.org/10.1007/978-1-4757-1095-3

17. A. El-shenawy, M. El-Gamel, D. Reda, Troesch's problem: A numerical study with cubic trigonometric B-spline method, *Partial Differ. Equ. Appl. Math.*, **10** (2024), 100694.

18. M. El-Gamel, A. El-Shenawy, A numerical solution of Blasius equation on a semi-infinity flat plate, *SeMA*, **75** (2018), 475–484. https://doi.org/10.1007/s40324-017-0145-x

19. K. A. Aldwoah, M. A. Almalahi, M. Hleili, F. A. Alqarni, E. S. Aly, K. Shah, Analytical study of a modified-ABC fractional order breast cancer model, *J. Appl. Math. Comput.*, **70** (2024), 3685–3716. https://doi.org/10.1007/s12190-024-02102-7

20. H. Khan, J. Alzabut, A. Shah, Z. He, S. Etemad, S. Rezapour, et al., On fractal-fractional waterborne disease model: A study on theoretical and numerical aspects of solutions via simulations, *Fractals*, **31** (2023), 2340055. https://doi.org/10.1142/S0218348X23400558

21. A. E. Hamza, O. Osman, A. Ali, A. Alsulami, K. Aldwoah, A. Mustafa, et al., Fractal-fractional-order modeling of liver fibrosis disease and its mathematical results with subinterval transitions, *Fractal Fract.*, **8** (2024), 638. https://doi.org/10.3390/fractalfract8110638

22. T. Alraqad, M. A. Almalahi, N. Mohammed, A. Alahmade, K. A. Aldwoah, H. Saber, Modeling Ebola dynamics with a Φ-piecewise hybrid fractional derivative approach, *Fractal Fract.*, **8** (2024), 596. https://doi.org/10.3390/fractalfract8100596

23. A. Carpinteri, P. Cornetti, A. Sapora, A fractional calculus approach to nonlocal elasticity, *Eur. Phys. J. Spec. Top.*, **193** (2011), 193–204. https://doi.org/10.1140/epjst/e2011-01391-5

24. D. Baleanu, Y. Karaca, L. Vázquez, J. E. Macías-Díaz, Advanced fractional calculus, differential equations and neural networks: Analysis, modeling and numerical computations, *Phys. Scr.*, **98** (2023), 110201. https://doi.org/10.1088/1402-4896/acfe73

25. M. S. Algolam, O. Osman, A. Ali, A. Mustafa, K. Aldwoah, A. Alsulami, Fixed point and stability analysis of a tripled system of nonlinear fractional differential equations with n-nonlinear terms, *Fractal Fract.*, **8** (2024), 697. https://doi.org/10.3390/fractalfract8120697

26. Y. A. Rossikhin, M. V. Shitikova, Application of fractional calculus for dynamic problems of solid mechanics: Novel trends and recent results, *Appl. Mech. Rev.*, **63** (2010), 010801. https://doi.org/10.1115/1.4000563

27. M. Caputo, M. Fabrizio, A new definition of fractional derivative without singular kernel, *Progr. Fract. Differ. Appl.*, **1** (2015), 73–85.

28. A. Atangana, Fractal-fractional differentiation and integration: Connecting fractal calculus and fractional calculus to predict complex system, *Chaos Soliton Fract.*, **102** (2017), 396–406. https://doi.org/10.1016/j.chaos.2017.04.027

29. K. Shah, T. Abdeljawad, Study of radioactive decay process of uranium atoms via fractals-fractional analysis, *S. Afr. J. Chem. Eng.*, **48** (2024), 63–70. https://doi.org/10.1016/j.sajce.2024.01.003

30. A. Shah, H. Khan, M. De la Sen, J. Alzabut, S. Etemad, C. T. Deressa, et al., On non-symmetric fractal-fractional modeling for ice smoking: Mathematical analysis of solutions, *Symmetry*, **15** (2023), 87. https://doi.org/10.3390/sym15010087

31. D. Bainov, P. Simenonv, *Impulsive differential equations: Periodic solutions and applications*, Routledge, 1993.

32. T. A. Burton, A fixed-point theorem of Krasnoselskii, *Appl. Math. Lett.*, **11** (1998), 85–88. https://doi.org/10.1016/S0893-9659(97)00138-9

33. R. Singh, J. Mishra, V. K. Gupta, Dynamical analysis of a tumor growth model under the effect of fractal fractional Caputo-Fabrizio derivative, *Int. J. Math. Comput. Eng.*, **1** (2023), 115–126. https://doi.org/10.2478/ijmce-2023-0009

AIMS Press